This paper was presented at the 21st Wind & Solar Integration Workshop (2022) and published in the workshop's proceedings

ANALYSIS OF TRANSIENT STABILITY OF GENERATOR GROUPS IN THE FUTURE POWER SYSTEM

Daniel Scheifele* , Hendrik Lens

University of Stuttgart, Stuttgart, Germany
**E-mail: daniel.scheifele@ifk.uni-stuttgart.de*

Keywords: POWER SYSTEM STABILITY, POWER SYSTEM DYNAMICS, TRANSIENT STABILITY, ENERGY TRANSITION, CRITICAL FAULT CLEARING TIME

Abstract

Transient stability is an essential property of electrical power systems. It describes the ability of the system to maintain synchronous operation of all generators. Classically, transient stability of individual generators is analyzed based on possible loss of synchronism after near short-circuit faults. In contrast, this paper considers transient stability of generator groups as a potential instability phenomenon in future grid scenarios. We investigate and analyze relevant factors of influence and countermeasures and modeling aspects to consider when studying the phenomenon. Based thereon we discuss the effectiveness of possible countermeasures. The main focus of this paper is to provide a better understanding of the underlying dependencies within the power system and their impact on the stability itself.

1 Introduction

The increasing penetration of renewable energy sources (RES) in the context of the European energy transition leads to highly changed feed-in and power flow situations in the continental European (CE) electricity grid. In this context, it is of great relevance for system stability that installed wind and PV plants are connected to the grid via converters instead of synchronous machines like conventional power plants. This leads to the fact that, since RES do not contribute to system inertia yet, both the amount and the distribution of inertia in the system highly depend on the feed-in situation. Furthermore, expected future distribution of generation capacities (especially due to the addition of wind turbines near the coast or offshore) and growing international power trading volumes result in increasing power transits [1, 2].
Transient stability of an individual synchronous generator is a well-known and well-understood issue [3, 4]. Simulations of the German TSO for future grid scenarios show that, driven by the conditions described above, transient stability problems can occur that affect coherent generator groups [1, 5]. This means that entire grid regions can lose synchronism with the rest of the grid, which ultimately results in the affected area being disconnected by distance protection. This leads to undesired system split scenarios and small grid regions with high active power imbalance and high blackout risk. As already described in [6], this type of transient stability strongly depends on external factors such as the overall load flow scenario, the level and distribution of inertia, dynamic reactive power reserves and dynamic load behavior.
The work in [6] represents the methodological and content-related basis for this study. It describes the phenomenon and explains how it plays an increasingly important role for power system stability in the context of the energy transition. It also presents the grid model and explains the methodology for the investigations. In this work, further relevant factors of influence on transient stability of generator groups and modeling aspects are investigated.
In the following, a brief summary of the methodology is given. Subsequently, several other relevant characteristics are explained and described in more detail. The goal is to gain a better understanding for underlying dependencies between power transfer, inertia distribution, dynamic load behavior and dynamic reactive power reserves and to point out sensitivities for modeling aspects.

2 Methodology

2.1 Grid Model

As described in [6], the following investigations are based on RMS simulations with a simple 8-node grid model in the software *PowerFactory*. The model represents the most important characteristics of the German transmission system (i.e. high renewable feed-in in the north, load centers in the south and west and the rough geographic dimension). On the other hand, it is consciously chosen as simple as possible to ensure that all relevant cause-effect-relations can be easily determined and adequately analyzed.
Figure 1 shows the schematic 'six plus two' node grid model consisting of six nodes with generation and consumption (larger dots in the figure) and two nodes without in the north-south transfer region that ensure realistic grid meshing, which is characteristic for the real German transmission grid. This

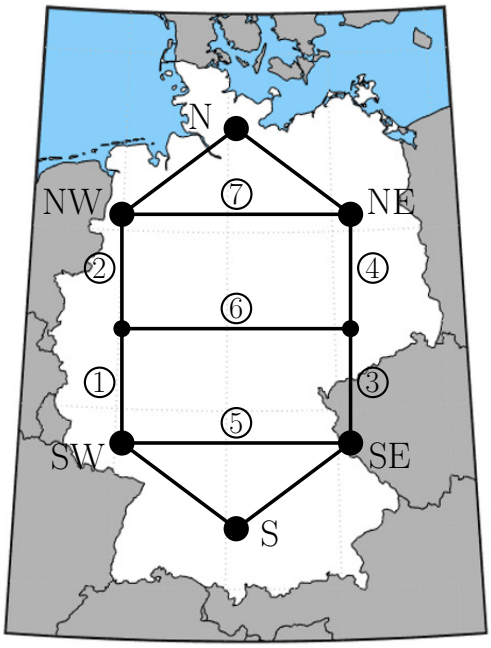

Fig. 1 Illustration of the simplified German power grid used for the investigations.

model mainly consists of two regions ('north' and 'south') with three nodes each. This means that, in case of a fault, at one of the edges 1-7 within the north-south transfer region, there is a certain amount of generation and consumption close to the fault while the rest is further away. Generally, it is expected that grid topology assumptions and also the boundary grid may have a huge impact on the overall results. Further information about modeling aspects and grid parameters can be found in [6].

2.2 Method for Investigation

Within the investigations, all faults are assumed to be three-phase faults on the fault lines at the edges 1-7. As also described in [6], for each scenario the so-called 'critical fault clearing time' (CCT), being the shortest fault clearing time for which any generator loses synchronism, is used to evaluate the criticality of a grid scenario: The smaller the minimum CCT over all fault locations, the more critical the overall scenario is. The CCT calculation was done with a bisectional iteration for each relevant fault line with a resolution of 1 ms and a maximal relevant CCT of 1000 ms.

3 Results

For the investigations, a pre-fault load flow 'basic scenario' was chosen which is to be expected in the future. The scenario especially includes a high share of converter-based feed-in ($\sim$87 %) leading to high power transfer from north to south ($\sim$15 GW). The high share of renewable generation also leads to the fact that only a few synchronous generators (SG) remain

Table 1 CCT for different transit scenarios in ms. Missing entries correspond to CCT $>$ 1000 ms.

edge	transit scenario (N-S)		
	13 GW	15 GW	17 GW
1	553	304	172
2	-	412	180
3	568	310	176
4	-	467	172
5	-	419	236
6	848	336	185
7	-	-	-

(15 GVA installed capacity) leading to decreasing dynamic reactive power reserves during and after faults. Due to the high power transfer, there is a need for static reactive power compensation systems to keep the pre-fault-voltages in the admissible range. For the sake of simulation performance, static capacitors with 6 Gvar nominal reactive power in total are used. In the simulations all RES units are connected to the grid via grid-following converters.
The comparison between different scenarios was done by modifying only one parameter at a time. This ensures that the impact of a parameter can be investigated individually.

3.1 Factors of influence

As already described in [6], three indicators have been found to be particularly relevant for transient stability of generator groups:

- total power transfer between the two regions,
- total availability of synchronous generators and their distance to the fault location,
- ratio of the respective inertia of the two regions.

In the following, the impact of total power transfer between the two regions will be investigated in more detail. For power transfer variation, feed-in by RES is shifted from node 'S' to 'N' and vice versa. Table 1 shows the CCT for different transfer scenarios. The maximum clearing time valid in Germany for a so-called 'conceptually cleared fault' of 150 ms can be used as a comparative value at this point. It is clear to see that increasing power transit leads to area-wide smaller CCT and therefore to higher transient instability risks.

Figure 2 shows the results for a fault on edge 1 with a clearing time of 160 ms for three scenarios with different north-south power transfer. The plots show average frequencies and voltages for north (i.e. nodes N, NW, and NE) and south region (i.e. nodes S, SW, and SE), the phase angle difference between the nodes 'N' and 'S' and the power transfer deviation between the two regions relative to the pre-fault steady-state.
The phase angle plots show the physical dependency between power transit and pre-fault phase angle differences. It is also shown that there is a larger power transfer deviation, resulting

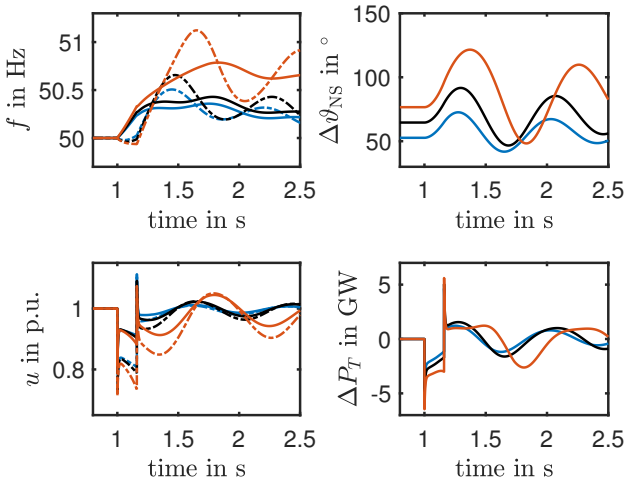

Fig. 2 Comparison of different transit scenarios **13 GW**, **15 GW** and **17 GW**. Average frequencies and voltages for the regions south (- -) and north (—), N-S voltage phase angle differences and active power transfer deviation ΔP_{T}.

in higher frequency gradients (especially in the northern region with high excess of active power). This leads to a much faster increase of the phase angle differences in scenarios with higher pre-fault transit and the two regions drifting further apart, leading to more critical system behavior (and therefore smaller CCT). The voltage plots reveal, that voltage restoration after the fault is poorer due to the higher reactive power demand (and limited dynamic reactive power reserves) as a result of larger active power imbalances.

Another relevant factor of influence is the ratio of the respective inertia of the two regions 'north' and 'south'. To examine this in more detail, the total amount of SG (15 GVA) as well as the number of SG near fault locations, i.e. at the nodes 'SE','SW','NE' and 'NW' (2 GVA at each node) stays constant. For the following investigations, the remaining SG with a total apparent power of 7 GVA are moved from node 'S' to 'N' and the corresponding RES units vice versa. Table 2 shows the resulting CCT for the three scenarios '1 GVA', '3.5 GVA' and '6 GVA', relating to the installed SG capacity at node 'N'. The '3.5 GVA' scenario is equal to the '15 GW transit' scenario in table 1.

The CCT show that the criticality of the overall scenario is reduced with increasing amount of SG at node 'N'. The underlying correlations are closely related to differences in the dynamic behavior of loads and RES and will now be analyzed in more detail.

Figure 3 shows different plots for a fault on edge 1 with a CCT of 200 ms. The frequency plot shows the expected frequency gradient increase due to the power imbalance after fault occurrence in scenarios with low SG availability at node N (with the same active power transfer deviation). This higher gradient leads to a higher increase in phase angle differences between the nodes 'N' and 'S'. Higher phase angle differences lead to higher power transfer related to re-synchronization after fault

Table 2 CCT for different N-S inertia inequality scenarios in ms. Missing entries correspond to CCT $>$ 1000 ms.

edge	SG apparent power at node N		
	1 GVA	3.5 GVA	6 GVA
1	227	304	516
2	254	412	922
3	229	310	527
4	237	467	-
5	338	419	-
6	245	336	486
7	-	-	-

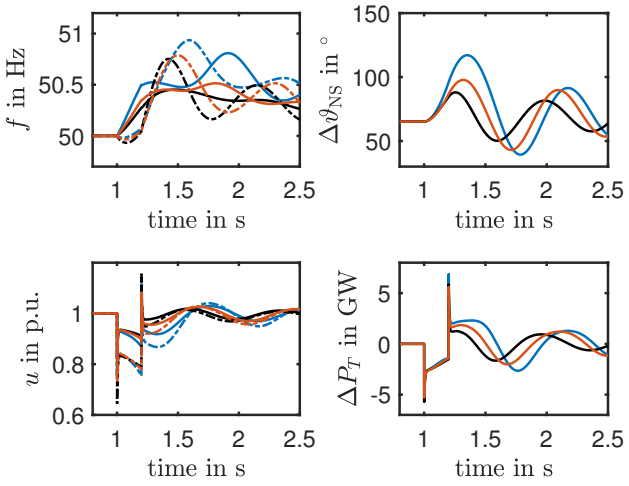

Fig. 3 Comparison of scenario with different N-S inertia inequality scenarios: **1 GVA**, **3.5 GVA** and **6 GVA** SG apparent power at node N. Average frequencies and voltages for the regions south (- -) and north (—), N-S voltage phase angle differences and active power transfer deviation ΔP_{T}.

clearing, causing poorer voltage recovery due to the limited amount of available dynamic reactive power reserves in the system. The active power imbalance in the southern region with active power import during the fault is additionally enlarged due to the underlying dynamic load behavior, which will be discussed later on.

In all simulations, RES utilization was assumed to be at 80% of the installed capacity as high RES feed-in is to be expected in critical future grid scenarios. In the following, the impact of the degree of RES utilization will be discussed in more detail. RES sources are mostly connected to the grid via converters, being very sensitive to over-current and therefore being equipped with over-current protection schemes. In the model, a maximal current of 1.05 p.u. is assumed. Additionally, dynamic reactive current feed-in is implemented as defined in the grid codes for fault ride through (FRT) support. The FRT gain was chosen to 2 p.u. reactive current/p.u. voltage deviation for the following simulations. The degree of utilization was varied by

Table 3 CCT for different degree of RES utilization in ms. Missing entries correspond to CCT > 1000 ms.

edge	RES utilization ($P_{\mathrm{RES,feed-in}}/P_{\mathrm{RES,installed}}$)		
	50%	95%	100%
1	527	262	273
2	-	299	312
3	531	263	275
4	-	301	321
5	612	304	315
6	712	334	352
7	-	-	-

changing the installed capacity of the RES units while holding their total active power feed-in constant. As a current limiting scheme, reactive current prioritization is implemented, leading to reduced active power feed-in in case of voltage drops.

Generally, a correlation between RES utilization factor and critical system behavior is to be expected. Table 3 shows the CCT for three scenarios with different degrees of RES utilization. The CCT given in the table show that there is a certain correlation between degree of RES utilization and the criticality of a scenario, but not over the full range between 50% and 100%. Moreover, the scenario with 100% utilization is not the expected 'worst-case' scenario w.r.t. transient stability.

The explanation for this unexpected observation is mainly caused by the nonlinear impact of current limiting. Figure 4 shows the results for the comparison of three scenarios after a fault on edge 1 with a CCT of 200 ms. Focusing on the plots for the 100% and for the 95% scenario, it shows that the reactive current prioritization leads to a curtailment of the active current in the 100% scenario, whereas in the 95% scenario the active current is enlarged to feed-in the desired active power into the grid. This leads to permanently higher power transfer (as seen in the curves for P_{T}) but to poorer voltage recovery due to the limited amount of dynamic reactive power compensation units. Thus, the nonlinear effect of current limiting may have a strong impact on transient stability, especially when there is a huge amount of RES feed-in. For real grid scenarios, the exact 'worst-case' RES utilization level is hard to estimate due to the fact that nonlinear correlations and different parameters play an important role.

As already mentioned, another relevant modeling aspect relates to dynamic load behavior. In general, dynamic load behavior highly influences transient stability, since large effects occur in the relevant time scale ($\sim$1s). However, dynamic load behavior is difficult to estimate in reality, particularly in case of large voltage deviations.
Figure 5 shows different plots for a fault on edge 1 with a clearing time of 200 ms and two different dynamic load modeling assumptions within the 'basic scenario': pure 'impedance load' behavior without dependency w.r.t frequency and 'mixed

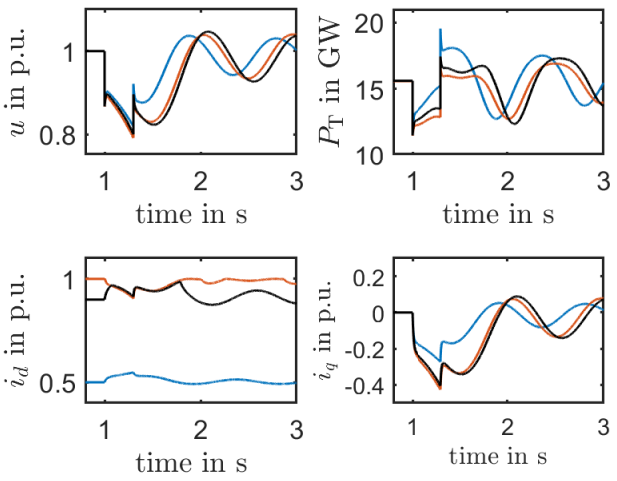

Fig. 4 Comparison of scenario with different RES utilization factors: **50%**, **100%** and **95%**. Bus voltage at node 'NE', active power transfer ΔP_{T} and active and reactive currents from RES unit at bus NE.

loads'. In all other simulations within this paper, 'mixed load' behavior is assumed, meaning a ZIP-model approach with equal shares of constant power, constant current and constant impedance load for voltage dependent behavior combined with a linear dependency w.r.t. frequency.
As described above, the plots show a high impact of dynamic load behavior on overall system dynamics and stability. Two main observations can be made: The scenario with impedance loads exhibits smaller voltage deviations but still larger deviations of load active power consumption (impedance loads exhibit a quadratic $P(U)$ dependency). This leads to a higher active power excess in the overall grid (resulting in higher frequency gradients), but the regions diverge more slowly (result in smaller phase angle differences). In the impedance load scenario, all CCT are larger than 1000 ms, meaning that there is no transient instability risk visible at all.

Generally, it can be said that the dynamic load behavior in the two regions 'south' and 'north' have a fundamentally different impact on system stability: The active power excess in the northern region during the fault is enlarged by the reduction of active power consumption as a result of the voltage drop. In the south, however, load behavior reduces existing active power imbalances due to the $P(U)$-behavior and thus improves transient stability. This dependency explains the enlarged active power imbalance in situations with high local availability of synchronous generators in the southern region as described in Figure 3. This general relationship should be taken into account when transient stability is investigated within grid simulations.

3.2 Countermeasures

Based on the indicators described above and as already described in [6], several countermeasures are potentially relevant to improve transient stability:

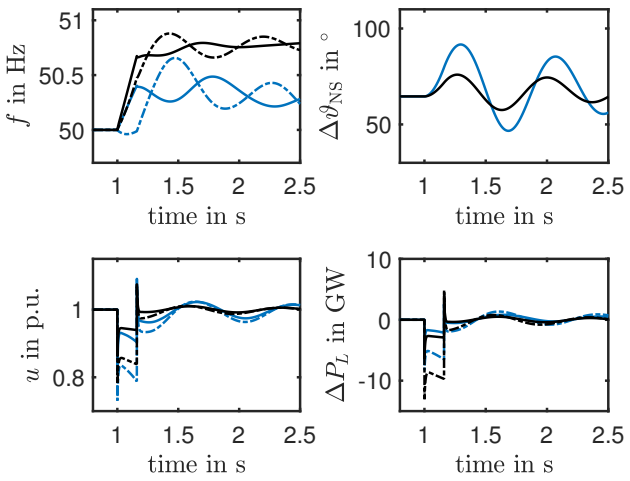

Fig. 5 Comparison of scenario with impedance load dynamics **(black)** and mixed loads **(blue)**. Average frequencies and voltages for the regions south (- -) and north (—), N-S voltage phase angle differences and load active power deviation ΔP_{L} from nominal value.

- fast frequency regulation mechanisms such as 'Fast Frequency Response' (FFR) and fast Limited Frequency Sensitive Mode (LFSM),
- dynamic reactive power compensation systems such as STATCOMs, 'Grid-forming Converters' (GFMC) or Synchronous Condensers (SC),
- additional HVDC transmission lines or power plant redispatch in order to reduce AC power transfer.

Some of the potential countermeasures are already described in the literature, e.g. the use of HVDC links [7] and GFC [8], but with a different focus and without referring to the underlying correlations and dependencies.

The idea of frequency regulation mechanisms is to reduce the local active power imbalances by adjusting the active power feed-in of power plants (especially RES). Generally, the simulations show that the impact of frequency regulation mechanisms is limited due to the relevant time range of ∼1s in which the instability phenomenon is observed. These mechanisms are not designed to adjust active power feed-in in such a small time range.

As already shown in [6], the effectiveness of STATCOM and SC as countermeasures highly depends on their respective location. The results especially show that seemingly obvious causal relationships (such as placement of SC improves system stability) may not be valid under certain conditions due to system inherent dependencies. It can be generally said that the placement of these systems needs to be individually examined and evaluated.

Additional HVDC transmission lines and power plant redispatch are used to reduce the overall AC power transfer, being the most important indicator for transient stability risks. Since power plant redispatch has only minor impact on overall system dynamics and is no longer expected to be available as a measure in the future energy system to the extent needed, it is not considered separately.

Table 4 CCT for different HVDC line usage scenarios in ms. Missing entries correspond to CCT $>$ 1000 ms.

edge	setpoint for P_{HVDC}		
	0 GW	2 GW	4 GW
1	256	384	495
2	282	571	-
3	260	386	525
4	280	-	-
5	375	563	711
6	273	427	659
7	-	-	-

In the following, the impact of HVDC transmission lines as a countermeasure is investigated in more detail. To this end two HVDC lines are implemented: one 'western' link between the nodes 'NW' and 'SW' and one 'eastern' link between the nodes 'NE' and 'SE'. All converters are modeled with an apparent power of 2 GVA and a maximum current of 1.1 p.u. for all scenarios. The placement of the converter stations close to possible fault locations allows for the investigation of the impact of current limiting due to FRT reactive current support in case of voltage drops. The FRT gain was chosen to 4 p.u./p.u. in the following scenarios. For HVDC modeling, a simplified model is used, neglecting protection schemes, DC-link chopper, $P(f)$ or $Q(U)$ adjustment controllers.

For the investigations, the 17 GW power transfer scenario, as the most critical scenario w.r.t. transient stability, was used as a base scenario. In the following, the DC power transfer over the two HVDC lines is varied: In the first scenario, the two HVDC lines are active but with a set-point of 0 GW. In the second scenario, the set-points are 1 GW per line and in the third scenario, the HVDC lines are used at full load corresponding to a total DC power transfer of 4 GW.
Table 4 shows the resulting CCT on the edges 1-7 for the different scenarios. The remaining AC power transits for the three scenarios are related to the three different power transfer scenarios from Table 1 (with power transits of 13, 15 and 17 GW), but with additional reactive power reserves in case of voltage drops from the HVDC converters. Generally, an area-wide stability improvement can be observed through the increased use of HVDC links. Additionally, when comparing the CCT values with those in Table 1, the positive impact of the reactive power provision becomes visible. As an example, the CCT value of edge 1 increase from 172 ms to 256 ms when adding an HVDC link that is operated at 0 GW.

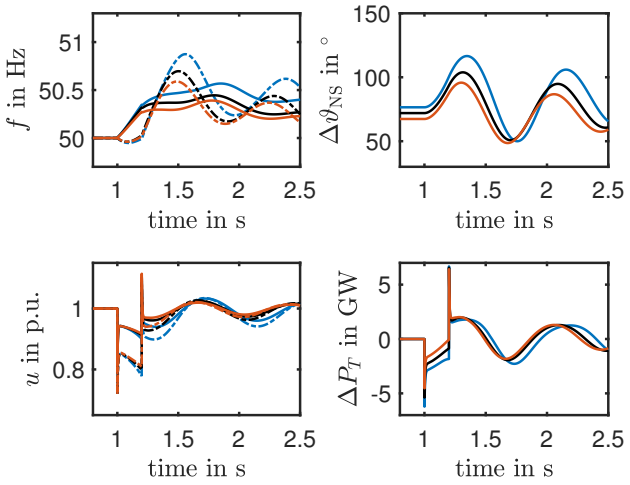

Fig. 6 Comparison of different HVDC usage scenarios **'0 GW'**, **'2 GW'** and **'4 GW'**. Average frequencies and voltages for the regions south (- -) and north (—), N-S voltage phase angle differences and active power transfer deviation ΔP_{T}.

Figure 6 shows the results for the three different HVDC usage scenarios after a fault on edge 1 with a clearing time of 200 ms. The plots show two main effects of the reduced AC transit by using HVDC links: both the pre-fault phase angle difference and the active power imbalance during the fault are reduced. The former leads to a larger stability margin, while the latter leads to smaller frequency gradients and smaller increase of the phase angle difference. Due to the smaller active power imbalances there is a lower demand for reactive power, leading to better voltage recovery after fault clearing and therefore to improved stability in the overall scenario.

In can be concluded that the usage of HVDC links improves transient stability both by reducing the remaining AC active power transit and by providing additional reactive power in case of large voltage deviations. Hence, HVDC links can be seen as a suitable countermeasure for the expected problems related to transient stability in future grid scenarios.

4 Conclusion

The results show that the instability phenomena described by the German TSO in future grid scenarios are reproducible by a simple grid model. The investigations within this paper show that risks w.r.t. transient stability of generator groups is to be expected in grid situations with high area-wide power transfer as well as unfavorable inertia distribution. Driven by large scale feed-in of wind power near the coast or offshore, relevant grid scenarios are to be expected to occur more frequently in the future. In order to understand the underlying stability problem and to analyze adequate countermeasures, it is important to understand the causalities between power transfer, inertia distribution, dynamic load behavior, dynamic reactive power reserves as well as current limiting schemes in RES. As shown above, an effective countermeasure is the installation of HVDC lines reducing the AC transit and thus the main factor influencing transient stability risks. Another effective countermeasure is to provide additional dynamic reactive power reserves to partially compensate for the expected reduction of synchronous generators. Further steps to improve the investigations include taking the surrounding transmission systems into account by the integration of the presented grid model into a simplified CE grid model in order to confirm the results or to identify further relevant factors of influence and correlations.

5 Acknowledgements

The support of this study by the working group 'System Stability' of the four German TSO is gratefully acknowledged.

6 References

[1] 50Hertz, Amprion, TenneT, TransnetBW, "Grid development plan 2035". Accessed Sept. 02 2022 [Online]. Available: https://www.netzentwicklungsplan.de/sites/default/files/paragraphs-files/NEP2035_Bestaetigung.pdf

[2] ENTSO-E., "Ten year network development plan (TYNDP) 2020". Accessed Sept. 02 2022 [Online]. Available: https://eepublicdownloads.blob.core.windows.net/public-cdn-container/tyndp-documents/TYNDP2020/FINAL/entso-e_TYNDP2020_IoSN_Main-Report_2108.pdf

[3] P. Kundur, "Power system stability and control". The EPRI power system engineering series. *McGraw-Hill Inc*, 1994.

[4] N. Hatziargyriou, J. Milanovic, C. Rahmann, V. Vittal, "Definition and classification of power system stability – revisited & extended", *IEEE Transactions on Power Systems*, 2021, **36**, (4), pp. 3271–3281.

[5] N. Kalloe, J. Bos, J. Rueda Torres, "A fundamental study on the transient stability of power systems with high shares of solar PV plants", *Electricity*, 2020, **1**, pp. 62–86.

[6] D. Scheifele, H. Lens, "Transient stability of generator groups - factors of influence and countermeasures", *NEIS 2022; Conference on Sustainable Energy Supply and Energy Storage Systems*, 2022 (accepted).

[7] L. Sigrist, F. Echavarren, L. Rouco, "A fundamental study on the impact of HVDC lines on transient stability of power systems", *IEEE Eindhoven PowerTech*, 2015. pp. 1–6.

[8] Rokrok, E., Qoria, T., Bruyere, A., "Transient stability assessment and enhancement of grid-forming converters embedding current reference saturation as current limiting strategy", *IEEE Transactions on Power Systems*, 2022, **37**, (2), pp. 1519–1531.